Meteoroid flux determination using image intensified video camera data from the CILBO double station

Theresa Ott[1], Esther Drolshagen[1], Detlef Koschny[2], Gerhard Drolshagen[2], Bjoern Poppe[1]

[1] **University of Oldenburg, Oldenburg, Germany**
Theresa.Ott@uni-oldenburg.de, Esther.Drolshagen@uni-oldenburg.de,
Bjoern.Poppe@uni-oldenburg.de

[2] **European Space Agency, ESTEC, Noordwijk, The Netherlands**
Detlef.Koschny@esa.int, Gerhard.Drolshagen@esa.int

The double-station meteor camera setup on the Canary Islands, called CILBO, has been active since July 2011. This paper is based on the meteor data of one year (1.6.2013 – 31.5.2014). As a first step the statistical distribution of all observed meteors from both cameras was analyzed. Parameters under investigation include: the number of meteors observed by either one or both cameras as a function of the months, magnitude and direction. In a second step the absolute magnitude was calculated. It was found that ICC9 (La Palma) detects about 15% more meteors than ICC7 (Tenerife). A difference in the camera setting will be ruled out as a reason but different pointing directions are taken into consideration. ICC7 looks to the north-west and ICC9 looks to the south-east. A suggestion was that ICC9 sees more of the meteors originating from the Apex contribution in the early morning hours. An equation by Verniani (1973) has been used to convert brightness and velocity to the mass of the incident particle. This paper presents first results of the meteor flux analysis and compares the CILBO flux to well-known reference models (Grün et al., 1985) and (Halliday et al., 1996). It was found that the measured CILBO data yield a flux which fits the reference model from Grün et al. quite well.

1 Introduction

The CILBO (**C**anary **I**sland **L**ong-**B**aseline **O**bservatory) setup on the Canary Island has been active since July 2011. For this paper the collected data of one year, between 1 June 2013 and 31 May 2014, is used. In this year ICC7 collected 18398 meteors and ICC9 21158. Of these, 6663 meteors were detected simultaneously by both cameras.

The two camera stations are fully automated. One is located on Tenerife and one on La Palma on the Canary Islands. Each station hosts an image-intensified video camera, ICC (Intensified CCD Camera). The ICCs reach a limiting stellar magnitude of about +7.0. The camera on Tenerife is called ICC7, the one on La Palma ICC9. They are pointed at the same point in the sky in 100 km altitude, resulting in an overlap volume of the two observation volumes which is covered by both cameras. Due to this, it is possible to calculate the trajectory of the meteors observed simultaneously by both cameras in the overlap volume. *Figure 1* shows a sketch of the CILBO setup generated using Google Earth.

If the weather permits it, the system switches on. Every night the data is collected and transferred via ftp to a central server. The meteors are being observed using video data, therefore a meteor is visible on a varying number of single frames. The software *MetRec* (Molau, 1999) accesses the video data of the single stations and examines them in order to find meteors. For more information about the CILBO setup see Koschny et al. (2013) Furthermore, for a more detailed description of the data set and how to avoid mistakes using similar setups see Koschny et al. (2014).

For this paper the CILBO data of one year is presented. First, the magnitude distribution was examined. It has been found that ICC9 sees about 15% more meteors than ICC7. Differences in the settings will be analyzed more closely and ruled out as a reason for this discrepancy. A suggestion was that ICC9, looking to the East, sees more of meteors originating from the Apex contribution in the early morning hours. The mass distribution of the one year data set is presented, as well as the derived flux.

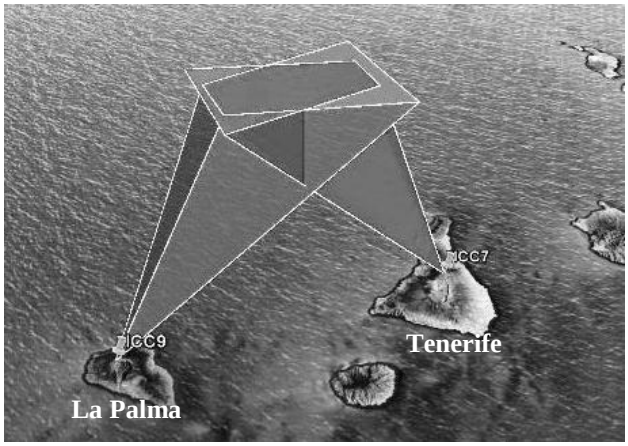

Figure 1 – Sketch of the CILBO system. The field of view of both cameras with an overlap volume covered by both cameras up to a height of 100 km. On the right is the ICC7 on Tenerife and on the left the ICC9 on La Palma.

2 The magnitude distribution

Every night a *.log file is generated by *MetRec* for both stations. This file lists information of each detected meteor. It includes, amongst others, the brightness of the meteor, its angular velocity and its type (shower or sporadic). The single-station data yield a magnitude value

calculated by *MetRec* for every meteor. In *Figure 2* the number of detected meteors in one year over their magnitude is plotted. The striped bars are the meteors collected only by ICC7 (Tenerife). The dotted bars are the meteors detected only by ICC9 (La Palma). The grey bars are the meteors observed by both cameras simultaneously. The utilized magnitudes are the mean values between the magnitudes determined by ICC7 and by ICC9. This first analysis of the data indicates that ICC9 sees more and fainter meteors than ICC7. The maximum of the ICC7 meteor distribution is at a magnitude of +3.5, the maximum of the ICC9 distribution is at +4.0 mag. This suggests that ICC9 is more sensitive than ICC7. This discrepancy will be examined in the following sections.

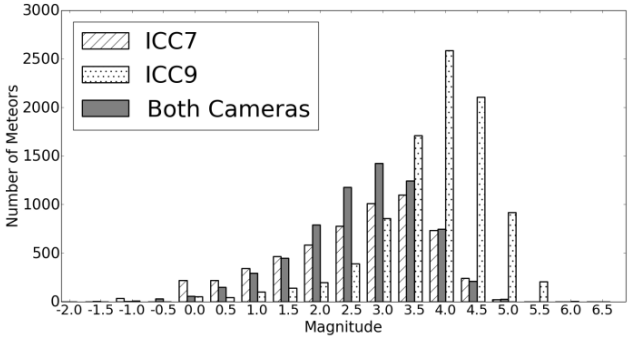

Figure 2 – Magnitude distribution of the CILBO data for one year. White, striped bars: Meteors detected only by ICC7. White, dotted bars: Meteors detected only by ICC9. Grey bars: Meteors detected simultaneously by both cameras.

3 The limiting magnitude

To analyze this difference in detection probability the *.log files have to be examined more closely. Every night *MetRec* determines the limiting magnitude by comparing the detected magnitude of reference stars with their real magnitude. In each *.log file the photometric equation, the color index correction, and the nominal limiting magnitude of the corresponding night are listed. The equations were extracted from the files and an average of the analyzed year is determined. These averaged equations are listed in *Table 1*. This yields a limiting magnitude of +6.64 for ICC7 and +6.29 for ICC9. According to this the ICC7 should detect fainter meteors.

Table 1 – The average photometric equation, color index correction and limiting magnitude of the cameras for data of one year.

	ICC7	ICC9
Photometric equation	$\mathbf{-2.39 \cdot log(pixelsum) + 9.45}$	$\mathbf{-2.31 \cdot log(pixelsum) + 9.02}$
Color index correction	$\mathbf{-0.33 \cdot (B-V) + 0.25}$	$\mathbf{-0.3 \cdot (B-V) + 0.19}$
Nominal lim. magnitude	$\mathbf{6.64\ mag}$	$\mathbf{6.29\ mag}$

4 The absolute magnitude

The absolute magnitude is the magnitude a meteor would have, if it would be in 100 km height in the observer's zenith. The information needed to calculate the absolute magnitude is taken from *.daf files (detailed altitude file) generated by the software *MOTS* (Meteor Orbit and Trajectory Software), see Koschny and Diaz del Rio (2002). An exemplary *.daf file is presented in *Figure 6*. The figure shows the information about one meteor observed simultaneously by both cameras on 07.08.2013 at $01^h44^m06^s$. It was recorded by both cameras on 19 frames. Information about the double-station meteor as seen by one station is listed for each frame on which the meteor was detected. *Figure 6* includes the consecutive number of the frame in the first column. The second column shows the time when the image was taken, in decimal seconds. In the third column of *Figure 6* the apparent magnitudes are listed. The next entries present the relative x and y positions of the meteor with respect to the center of the field of view. The height of the meteor above the Earth's surface with an error estimate is registered in the columns six and seven. The point directly under the meteor is specified in longitude and latitude. These values are also listed. In the columns 11 and 12 the meteor's distance to the camera in meters with an error estimate are presented. The velocity of the meteor, calculated for that video frame and the former one, with an error estimate are entered into the last two columns.

Another program has checked all *.daf files and deleted every file with unphysical entries, for example files that include negative values of velocity or altitudes. In the analyzed year 6663 simultaneously observed meteors were recorded. The control program declared 6132 of them as usable.

The brightness values are extracted from the *.daf file (Column 3 in *Figure 6*). The brightest values of ICC7 and ICC9 are determined separately and named m_{obs} (observed magnitude). Additionally, the corresponding distance between meteor and camera d is obtained. In the case of multiple frames with the same, smallest magnitude value, the one corresponding to the shortest distance to the camera is taken. From the obtained magnitude data, the difference between the camera's magnitudes as well as a mean value are calculated. The plot in *Figure 3* shows the magnitude difference $(m_{ICC7} - m_{ICC9})$ over the mean magnitude.

In the next step the apparent magnitude is corrected to the absolute magnitude. For that the following equation is utilized.

$$m_{100} = m_{obs} + 2.5 \cdot \log_{10}\left(\frac{(100km)^2}{d^2}\right) \qquad (1)$$

With m_{obs} as the observed magnitude, d as the distance to the camera extracted from the *.daf files and m_{100} is the absolute magnitude. Additionally, it is necessary to correct the magnitude to account for atmospheric extinction *k*. Because of the already quite large

uncertainty in the brightness values a *k*-value for a zenith angle of 50° may be used. A table from Green (1992) yields an extinction value of $k = 0.25$. This corrected magnitude is calculated for both stations. The magnitude difference between the two station's corrected magnitudes $(m_{corr,ICC7} - m_{corr,ICC9})$ as well as the mean magnitude is derived. In *Figure 4* the magnitude difference is plotted over the mean magnitude of the absolute magnitude values. To compare the apparent and absolute magnitude *Figure 3* and *Figure 4* were evaluated. In both pictures the average magnitude difference is given and yields a first impression of the correction quality. The average apparent magnitude difference is $\Delta m_{app} = -0.44$ mag and the average absolute magnitude is $\Delta m_{abs} = -0.50$ mag. The standard deviation is 1.09, respectively 1.11. A further look at the graphs reveals that the corrected values are shifted to the left. This effect has been expected since most detected meteors were further away from the camera than 100 km. Therefore, a correction would reveal that they appear fainter than at 100 km. Due to the fact that the magnitude difference is computed using $m_{ICC7} - m_{ICC9}$ and that the mean difference value is negative, it can be assumed that the camera on La Palma, ICC9, categorizes the same meteor fainter than ICC7 does. The difference in the magnitude determination is shown later to be an effect of the settings of the detection software.

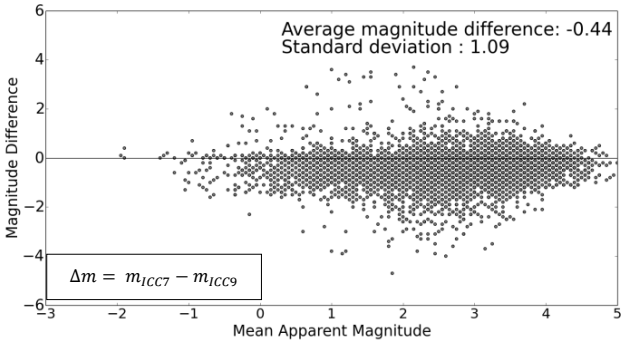

Figure 3 – Magnitude difference over the mean magnitude derived from the apparent magnitude values.

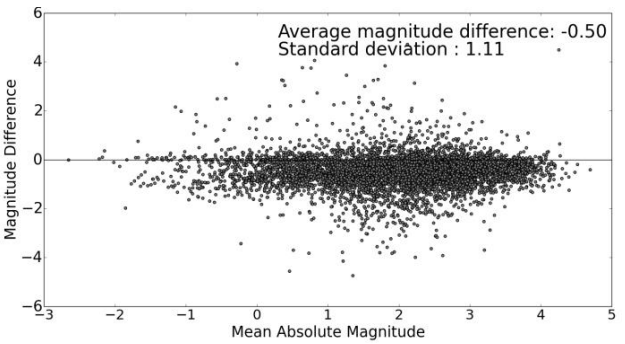

Figure 4 – Magnitude difference over the mean magnitude derived from the absolute magnitude values.

In *Figure 5* the plots from Section 2 are redone with a correction for the magnitude of ICC9. To accomplish that the difference of 0.44 mag is subtracted from the magnitude values of ICC9 to modify the brightness categorization. It is obvious that the magnitudes of ICC9 are now shifted to brighter values. Evidently, ICC9 does not detect fainter meteors than ICC7. Nonetheless ICC9 detected about 15% more meteors than ICC7 in the analyzed year.

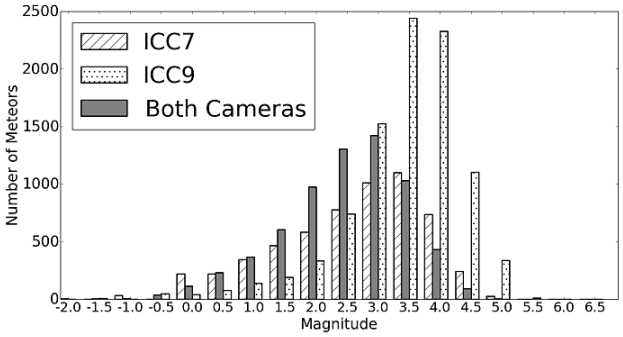

Figure 5 – Number of meteors as a function of their magnitude, whereas the ICC9 magnitude values are corrected by 0.44 mag. White, striped bars: Meteors detected only by ICC7. White, dotted bars: Meteors detected only by ICC9. Grey bars: Meteors detected simultaneously by both cameras.

5 Active times

It has to be taken into account that the cameras were not active the same amount of time. They are located on different islands and can only detect under good weather and sky conditions. The weather conditions may vary on the two islands. Furthermore, the cameras are pointed to the same position in the sky from different observation sites. Due to this they cover two different sides of the sky and the influence of the moonlight is not the same for the two cameras.

To diminish the effect of different active times on the number of recorded meteors an hourly rate is computed. For that the number of detected meteors is divided by the active time of the camera and converted to meteors per hour. The active times were determined by calculating the time between turning the camera on at the beginning of the night and off at the end. Off-times due to poor weather conditions were also taken into consideration. The hourly rate was determined for every night of the analyzed year and a monthly average was calculated. The distribution of the average hourly rate of every month for ICC7 and ICC9 is shown in *Figure 7*. The error bars are the standard deviation from the daily hourly rates in one month. It is evident that the rates of ICC9 are higher than those of ICC7. On average ICC9 detects 2 meteors more per hour than ICC7 does.

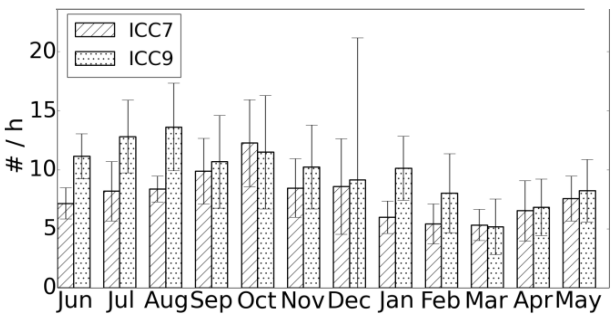

Figure 6 – Monthly average of the hourly rates of ICC7 (striped) and ICC9 (dotted) with error bars.

```
Station 1 - ICC7 - Tenerife
LogFile: 20130806.log
AppearanceDate: 07.08.2013
AppearanceTime: 01:44:06
INFFilename: 014406.inf
FrameCount: 19

!                    Position        Altitude in m           SubPoint        Cam. dist in m  Velocity in km/s
!###   Time  Bright   x      y       h       h  pos   lon/deg  lat/deg     dist   dist     v       v
 000  06.08    4.6  0.259  0.455  96245.1  ----.-    4.6   -17.192   28.385  115803.2  ----.-  --.---  --.---
 001  06.12    4.3  0.266  0.445  95481.0  ----.-    4.9   -17.192   28.389  115209.7  ----.-  21.675  --.---
 002  06.16    4.0  0.275  0.433  94614.0  ----.-   10.1   -17.192   28.394  114539.1  ----.-  25.856  --.---
 003  06.20    3.7  0.282  0.421  93793.7  ----.-    9.1   -17.192   28.398  113910.1  ----.-  23.269  --.---
 004  06.24    3.5  0.291  0.409  92903.3  ----.-    9.5   -17.192   28.403  113231.2  ----.-  26.556  --.---
 005  06.28    3.4  0.300  0.397  92054.8  ----.-    7.4   -17.191   28.407  112589.6  ----.-  25.307  --.---
 006  06.32    3.4  0.307  0.386  91264.3  ----.-    4.9   -17.191   28.412  111997.6  ----.-  22.427  --.---
 007  06.36    3.5  0.317  0.372  90357.4  ----.-   11.9   -17.191   28.416  111321.8  ----.-  27.054  --.---
 008  06.40    3.7  0.325  0.360  89518.4  ----.-    1.3   -17.191   28.421  110703.1  ----.-  23.804  --.---
 009  06.44    3.3  0.333  0.348  88720.8  ----.-    0.9   -17.191   28.425  110119.7  ----.-  23.793  --.---
 010  06.48    3.4  0.342  0.336  87900.0  ----.-   14.4   -17.190   28.429  109524.4  ----.-  23.292  --.---
 011  06.52    3.8  0.350  0.324  87116.5  ----.-    8.0   -17.190   28.433  108960.9  ----.-  23.378  --.---
 012  06.56    4.7  0.359  0.312  86308.5  ----.-   23.9   -17.190   28.438  108384.9  ----.-  22.931  --.---

Station 2 - ICC9 - La Palma
LogFile: 20130806.log
AppearanceDate: 07.08.2013
AppearanceTime: 01:44:06
INFFilename: 014406.inf
FrameCount: 19

!                    Position        Altitude in m           SubPoint        Cam. dist in m  Velocity in km/s
!###   Time  Bright   x      y       h       h  pos   lon/deg  lat/deg     dist   dist     v       v
 000  06.02    5.4  0.753  0.286  96780.4  ----.-    8.4   -17.192   28.383  123888.3  ----.-  --.---  --.---
 001  06.06    5.0  0.747  0.276  95845.2  ----.-   27.8   -17.192   28.388  122995.8  ----.-  25.894  --.---
 002  06.10    4.5  0.741  0.268  94970.6  ----.-   23.5   -17.192   28.392  122163.9  ----.-  26.082  --.---
 003  06.14    4.4  0.736  0.260  94223.0  ----.-    6.3   -17.192   28.396  121453.7  ----.-  22.295  --.---
 004  06.18    4.3  0.730  0.250  93327.5  ----.-   28.0   -17.192   28.401  120607.0  ----.-  25.404  --.---
 005  06.22    4.2  0.724  0.242  92484.9  ----.-   19.2   -17.191   28.405  119813.1  ----.-  25.128  --.---
 006  06.26    4.4  0.718  0.233  91637.7  ----.-   22.9   -17.191   28.410  119017.1  ----.-  24.037  --.---
 007  06.30    4.5  0.712  0.223  90779.4  ----.-   12.6   -17.191   28.414  118214.2  ----.-  25.601  --.---
 008  06.34    4.2  0.706  0.214  89952.7  ----.-   11.7   -17.191   28.418  117442.8  ----.-  23.456  --.---
 009  06.38    4.4  0.700  0.205  89138.2  ----.-    7.0   -17.191   28.423  116685.8  ----.-  24.298  --.---
 010  06.42    4.3  0.694  0.196  88336.2  ----.-    5.4   -17.191   28.427  115942.6  ----.-  22.756  --.---
 011  06.46    4.8  0.687  0.186  87425.2  ----.-   17.3   -17.190   28.432  115103.5  ----.-  27.177  --.---
 012  06.50    5.7  0.682  0.178  86760.7  ----.-    4.9   -17.190   28.435  114490.6  ----.-  18.858  --.---
```

Figure 7 – Exemplary *.daf file of a meteor observed simultaneously by both cameras on the 07.08.2013 at 01:44:06.

6 Corrected settings

After noticing the difference in the detection probability of ICC7 and ICC9 the detection software settings were examined. This revealed a difference in the configurations. ICC7 detected a meteor if it is recognizable on at least two frames. ICC9 needed three frames to register a meteor detection. This discrepancy has been corrected. Since June 2014 both cameras only detect a meteor if it is visible on at least three frames. Furthermore, a new reference star file was created using the tool RefStars from the *MetRec* software suite. This file sets up the relation between pixel value and magnitude. To find out if this was the reason for the higher detection rate of ICC9 the plots of Sections 2 and 5 are redone for June, July and half of August 2014 (compare *Figure 8* and *Figure 9*). In these months the configurations were adjusted. Unfortunately, there was a problem with the time synchronizing of the computers corresponding to the cameras. Therefore, there is no simultaneous meteor data yet.

Figure 8 shows the number of meteors over the magnitude. It is obvious that the brightness distribution is now the same for ICC7 and ICC9, although no magnitude correction was done. This is consistent with the assumption that the apparent sensitivity difference was the effect of the settings of the detection software. However, ICC9 still detects more meteors than ICC7. To compare this number difference *Figure 9* has been created. In this figure the average monthly hourly rate of the months with corrected settings is plotted. Nonetheless, on average ICC9 registered about 1.5 meteors more per hour than ICC7. It has to be taken into account that only data of three months was examined. To get significant results it is necessary to analyze more data

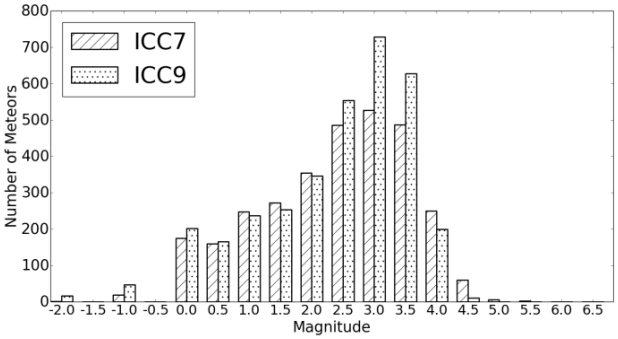

Figure 8 – Magnitude distribution of data form June, July and August 2014. The number of meteors observed by ICC7 is shown as striped bars. Those detected by ICC9 as dotted bars.

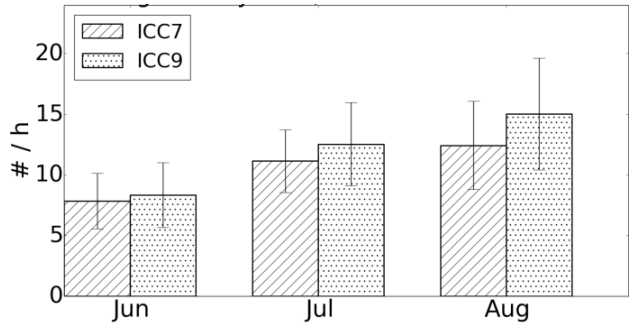

Figure 9 – Monthly average of the hourly rates of the three month data with corrected settings. ICC7: striped bars. ICC9: dotted bars.

with the new, corrected settings. However, the fact that ICC9 detects more meteors than ICC7 seems to be not an effect of the different settings and has to be analyzed more closely.

7 The viewing directions

It is now obvious that ICC9 detects more meteors than ICC7 over the same time period. Sensitivity differences between the cameras were found to not be a significant factor in the previous section. Furthermore, this difference cannot be traced back to longer observation times due to different weather conditions at one station because the hourly rates of the observing times were considered. Still, different detection settings cannot be ruled out as a reason until new data is analyzed.

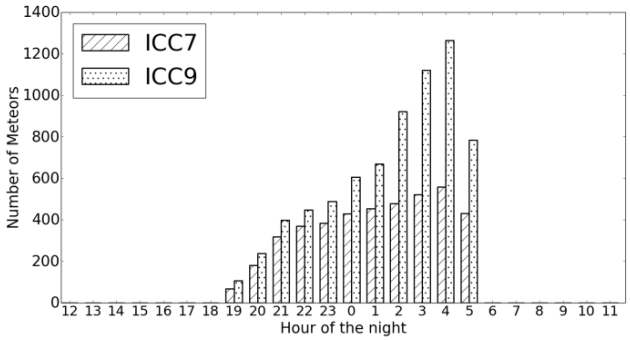

Figure 10 – Number of detected single-station meteors throughout the night. Meteors observed by ICC7 are shown as striped bars, those detected by ICC9 are presented as dotted bars.

If no further factors can be found for the discrepancy, it seems to be a result of the different viewing directions of the cameras (compare *Figure 1*). ICC7 is located on Tenerife and looks at the sky above La Palma. Accordingly, ICC7 looks to North-West. ICC9 is located on La Palma and looks to South-East.

In *Figure 10* the number of detected single-station meteors of one year is plotted over the hour of the night. It can be seen that ICC9 detects most of the meteors that it detects more than ICC7, in the early morning hours.

The fact that ICC9 sees more meteors than ICC7 can correspondingly be explained by its viewing direction. ICC9 is located on La Palma and looks to the East. In the East a lot of meteors can be detected in the early morning hours. This is due to the Apex contribution in the early morning hours, when the observer sees all the fast meteors orbiting the Sun in the opposite direction as the Earth. Therefore ICC7, looking to the West, detects a lot less meteors in those morning hours, than ICC9 does looking to the East.

8 The mass distribution

To calculate the mass of meteoroids corresponding to the recorded meteors a formula by Franco Verniani (1973) was used. His formula is the result of an analysis of about 6000 meteors recorded under the Harvard Radio Meteor Project. For his data Verniani found pre atmospheric meteoroid masses in the rage of 10^{-6} – 10^{-2}gram, whereas most of the meteoroid masses were found to be in an interval of $4 \cdot 10^{-6}$ – $4 \cdot 10^{-3}$gram. Furthermore, he computed a mean mass value of about 10^{-4} gram. From Verniani (1973) the following equation was extracted:

$$m = 63.71 - 10 \cdot \log(v) - 2.5 \cdot \log(M)$$
$$-2.5 \cdot \log(\cos(Z_R)) \qquad (2)$$

m is the absolute magnitude of the meteor at maximum light, v is the velocity, M is the meteoroid mass outside the Earth's atmosphere and Z_R is the zenith angle. For the CILBO data a mean zenith angle of $Z_R = 45°$ is assumed. The process of deriving the velocity is explained in Drolshagen et al. (2014) and the utilized absolute magnitude was averaged for both cameras. Solved for the mass the equation results in:

$$M = 10^{\frac{-m+64.09-10\cdot\log(v)}{2.5}} \qquad (3)$$

It has to be taken into account that Verniani's formula utilizes CGS-units. Due to this the velocity has to be stated in cm/s and the resulting mass is derived in grams. Furthermore, it has to be noted, that Verniani used the radio method for meteor detection. Therefore, he was able to detect fainter and consequently smaller meteors than those found by the video observing method. For example, about 50% of all his meteors had a magnitude between +8 and +9 whereas the CILBO system detected none in that magnitude interval.

In *Figure 11* the mass distribution resulting from the CILBO data of one year is shown. In this graph the axes are logarithmic. The masses are binned in 0.01 g bins and cumulatively plotted. It is obvious that most of the meteoroids are very small. 1769 meteors were created by meteoroids that fall into the first bin and have a mass under 0.01 g. This agrees with the expectations of very small meteoroids.

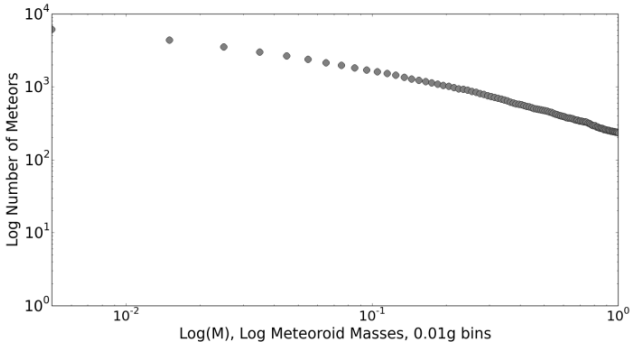

Figure 11 – Mass distribution of the CILBO data of one year calculated using Verniani's mass formula.

9 The flux

To determine the flux the area covered by both cameras in 100 km is needed (cross section of both fields of view at 100 km height). In *Figure 12* a top view of the area

covered by both cameras can be seen. The figure corresponds to a height of 100 km.

The areas of the field of view A in 100 km altitude of the cameras are:

$$A_{ICC7} = 3562.78\,\mathrm{km}^2, \qquad A_{ICC9} = 3878.91\,\mathrm{km}^2$$

And the shared field of view of the cameras is:

$$A_{Overlap} = 2943.71\,\mathrm{km}^2$$

To determine the flux of the double station observations the data of one year is utilized. With the calculated area covered by both cameras, the mass distribution, and the effective observing time $T = 1799.51$ h (the time when both cameras were simultaneously active in the analyzed year) it is possible to determine the flux F. The flux is the cumulative number of meteors per second and m^2 from meteoroids with masses equal to or bigger than M. In *Figure 13* the calculated flux is plotted. For this graph all double station meteors observed in one year are utilized. Furthermore, the theoretical flux curves derived from the models by Grün et al. (1985) and Halliday et al. (1996) are presented. The solid line shows the flux by Grün et al. and the dashed curve the flux by Halliday et al. The dots are the flux values resulting from the CILBO data. It is apparent that until a mass of about 1 g is reached the slope of the CILBO values is similar to the one calculated by Halliday et al. The flux for meteoroids smaller than 1 g is similar to predictions from the Grün et al. model. The decrease for higher masses does not match any of the curves. To compare the three models one has to keep in mind that Verniani has used radio observations for his studies. Due to this the mass formula might not be compatible with the utilized video measurements. Furthermore, it has to be taken into account that Grün's theory is a result of micro lunar crater data, infrared measurements of dust in space and in situ experiments and Halliday et al. have utilized only fireballs for their studies. Nevertheless, our flux values are in the same order as the ones calculated by Grün et al. and Halliday et al. and fit especially the Grün et al. model well.

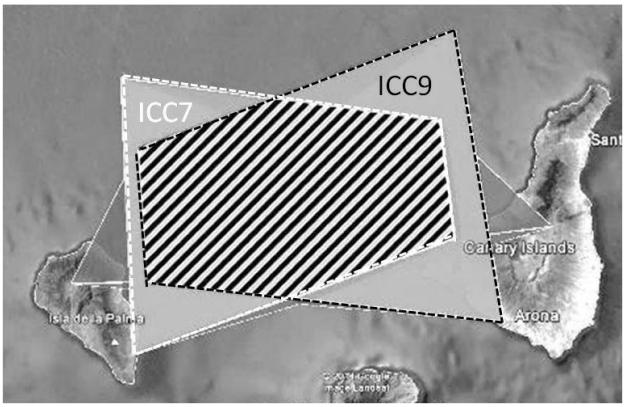

Figure 12 – Sketch of the area covered by both cameras (striped area). The cross section of the field of views at a height of 100 km above the Earth's surface is presented.

A closer look at *Figure 13* reveals a flux value for a meteoroid with a mass of 1 g or bigger of $10^{-14}\ Meteoroids/\mathrm{m}^2 \cdot s$. That means that at any given moment such a meteoroid can be found in a cube with edge length of 1000 km.

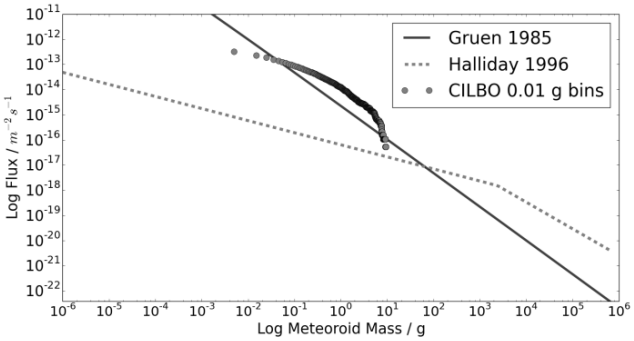

Figure 13 – Meteoroid flux: Number of meteoroids per m^2 and second with meteoroid masses equal to or bigger than M. Dots: The CILBO data flux, solid line: The flux according to Grün et al., dotted line: The flux derived by Halliday et al.

10 Conclusion and future work

The CILBO data collected in one year yield more than 6000 usable simultaneous meteor observations. The double-station data offers a lot of information about the magnitude, the direction and the flux of those meteors.

ICC9 detects about 15% more meteors than ICC7 in the analyzed year. Even after matching all settings the camera on La Palma records on average 1.5 meteors per hour more than the one on Tenerife. The viewing direction is probably one of the reason for the higher number of meteors detected by ICC9, looking towards East, than by ICC7 looking to the West. In the East a lot of meteors can be detected in the early morning hours. This is due to the Apex contribution of the early mornings, when the observer sees all the fast meteors orbiting the Sun in the opposite direction as the Earth. Nevertheless more systematic errors have to be uncovered.

The calculated masses were in the expected size category since a lot of the meteoroids which caused the meteors are smaller than 0.1 g. Despite that, the mass model should be adjusted from radar to video observations.

The computed flux from the CILBO data fits the Grün model well. At any given moment an exemplary meteoroid with a mass equal to or bigger than 1 g would be found in a cube with an edge length of 1000 km. However, the discrepancy of the in situ model or fireball model to actual video computations should be determined.

References

Drolshagen E., Ott T., Koschny D., Drolshagen G., and Poppe B. (2014). "Meteor velocity distribution from CILBO double station video camera data". In Rault J.-L., and Roggemans P., editors, *Proceedings of the International Meteor Conference*, Giron, France, 18–21 September 2014. IMO, pages ???–???.

Green D. (1992). "Magnitude Corrections for Atmospheric Extinction". *International Comet Quarterly*, **14**, 55–59.

Grün E., Zook H., Fechtig H., and Giese R. (1985). "Collisional Balance of the Meteoritic Complex". *Icarus*, **62**, 244–272.

Halliday I., Griffin A., and Blackwell A. (1996). "Detailed data for 259 fireballs from the Canadian camera network and inferences concerning the influx of large meteoroids". *Meteoritics and Planetary Science*, **31**, 185–217.

Koschny D., and Diaz del Rio J. (2002). "Meteor Orbit and Trajectory Software (MOTS) - Determining the Position of a Meteor with Respect to the Earth Using Data Collected with the Software MetRec". *WGN, the Journal of the IMO*, **30**, 87–101.

Koschny D., Bettonvil F., Licandro J., van der Luijt C., Mc Auliffe J., Smit H., Svedhem H., de Wit F., Witasse O., and Zender, J. (2013). "A double-station meteor camera setup in the Canary Islands – CILBO". *Geoscientific Instrumentation Methods and Data Systems*, **2**. 339–348.

Koschny D., Mc Auliffe J., Bettonvil F., Drolshagen E., Licandro J., van der Luijt C., Ott T., Smit H., Svedhem H., Witasse O., and Zender, J. (2014). "CILBO - Lessons learnt from a double-station meteor camera setup in the Canary Islands". In Rault J.-L., and Roggemans P., editors, *Proceedings of the International Meteor Conference*, Giron, France, 18–21 September 2014. IMO, pages ???–???.

Molau S. (1999). "The Meteor Detection Software MetRec". In, Baggaley W. J. and Porubcan V., Proceedings of the International Conference Meteoroids 1998, 17–21, 1998, Tatranska Lomnica, Slovakia, pages 131–134.

Verniani F. (1973). "An Analysis of the Physical Parameters of 5759 Faint Radio Meteors". *Journal of Geophysical Research*, **78**, 8429–8462.